ORIGINAL ARTICLE

Anti-inflammatory agent, OKN-007, reverses long-term neuroinflammatory responses in a rat encephalopathy model as assessed by multi-parametric MRI: implications for aging-associated neuroinflammation

Rheal A. Towner (ORCID) · **Debra Saunders** · **Nataliya Smith** ·
Rafal Gulej · **Tyler McKenzie** · **Brandy Lawrence** ·
Kathryn A. Morton

Abstract Lipopolysaccharide (LPS)–induced encephalopathy induces neuroinflammation. Long-term neuroinflammation is associated with aging and subsequent cognitive impairment (CI). We treated rats that had LPS-induced neuroinflammation with OKN-007, with an anti-inflammatory agent currently considered an anti-cancer investigational new drug in clinical trials for glioblastoma (GBM). Contrast-enhanced magnetic resonance imaging (MRI) (CE-MRI), perfusion MRI, and MR spectroscopy were used as methods to assess long-term (up to 6 weeks post-LPS) alterations in blood-brain barrier (BBB) permeability, microvascularity, and metabolism, respectively, and the therapeutic effect of OKN-007. A free radical–targeted molecular MRI approach was also used to detect the effect of OKN-007 on brain free radical levels at 24 h and 1 week post-LPS injection. OKN-007 was able to reduce BBB permeability in the cerebral cortex and hippocampus at 1 week post-LPS using CE-MRI. OKN-007 was able to restore vascular perfusion rates by reducing LPS-induced increased relative cerebral blood flow (rCBF) in the cortex and hippocampus regions at all time points studied (1, 3, and 6 weeks post-LPS). OKN-007 was also able to restore LPS-induced brain metabolite depletions. NAA/Cho, Cr/Cho, and Myo-Ins/Cho metabolite ratios at 1, 3, and 6 weeks post-LPS were all restored to normal levels following OKN-007 treatment. OKN-007 also reduced LPS-induced free radical levels at 24 h and 1 week post-LPS, as detected by free radical–targeted MRI. LPS-exposed rats were compared with saline-treated controls and LPS + OKN-007-treated animals. We clearly demonstrated that OKN-007 restores LPS-induced BBB dysfunction, impaired vascularity, and decreased brain metabolites, all long-term neuroinflammatory indicators, as well as decreases free radicals in a LPS-induced neuroinflammation model. OKN-007 should be considered an anti-inflammatory agent for age-associated neuroinflammation.

R. A. Towner · D. Saunders · N. Smith · R. Gulej ·
T. McKenzie · B. Lawrence
Advanced Magnetic Resonance Center, Oklahoma Medical
Research Foundation, 825 N.E. 13th Street, Oklahoma City, OK
73104, USA

R. A. Towner
Oklahoma Nathan Shock Aging Center, University of Oklahoma
Health Sciences Center, Oklahoma City, OK, USA

R. A. Towner (✉)
Oklahoma Center for Neuroscience, University of Oklahoma
Health Sciences Center, Oklahoma City, OK, USA
e-mail: Rheal-Towner@omrf.org

B. Lawrence
Center for Veterinary Health Sciences, Oklahoma State University,
Stillwater, OK, USA

K. A. Morton
Department of Radiology and Imaging Sciences, University of
Utah School of Medicine, Salt Lake City, UT, USA

🖄 Springer

Introduction

Systemic inflammation can induce long-lasting cognitive complications, particularly in association with aging, as implicated in several clinical and preclinical studies (Murray et al. 2012; Sun et al. 2015Cunningham and Hennessy, 2015; Yamanaka et al. 2017). It is well known that neuroinflammation has been long thought to be considered a risk factor for cognitive impairment (Sun et al. 2015; Yamanaka et al. 2017). In addition, cognitive impairment is associated as a direct outcome of aging (Bettio et al. 2017; Toth et al. 2017; Oedekoven et al. 2015). The lipopolysaccharide (LPS)–induced encephalopathy rodent model could be considered an accelerated aging model, due to the increased reported neuroinflammation and vasoconstriction (Towner et al. 2018). For instance, we previously demonstrated that magnetic resonance imaging (MRI) could be used to assess blood-brain barrier (BBB) disruption, vasoconstriction, increased free radical levels, and neuroinflammation-induced brain metabolite alterations (Towner et al. 2018). More specifically, contrast-enhanced MRI (CE-MRI) can provide quantitative data regarding disrupted BBB permeability, via measuring an increase in a MRI signal intensity due to the uptake of a MRI contrast agent, Gd-DTPA (gadolinium diethylene triamino penta acetic acid), which normally cannot cross the BBB in the brain. Perfusion MR imaging (pMRI) (e.g., arterial spin labeling (ASL)) can measure the relative cerebral blood flow (rCBF) that reflects pathology-associated alterations in tissue vascularity. Magnetic resonance spectroscopy (MRS) can be used to evaluate alterations in brain metabolite levels. In addition, free radical–targeted molecular-targeted MRI (mt-MRI) in combination with immuno-spin trapping (IST) can be used to quantitatively measure in vivo free radical levels associated with oxidative stress–related neuroinflammation. These same MRI indices can also be used to assess a therapeutic intervention that could inhibit or reverse neuroinflammation.

OKN-007 (OKlahoma Nitrone 007; 2,4-disulfophenyl-PBN (α-phenyl-t-butyl-N-nitrone); or disodium 4-[(tert-butyl-imino) methyl] benzene-1,3-disulfonate N-oxide or disufenton; also known as NXY-059) is a nitrone agent that has exhibited efficacy as a neuroprotectant (Clausen et al. 2008; Culot et al. 2009; Kuroda et al. 1999) and is involved in the inhibition of the upregulation of inducible nitric oxide synthase (Floyd et al. 2008). OKN also has anti-inflammatory and antioxidant properties (Floyd et al.

2008, 2011, 2013). OKN is a small molecule, which can be administered either intravenously or orally, is readily cleared, and has not been found to induce any adverse effects (Edenius et al. 2002; Lyden et al. 2007; Wemer et al. 2006) in over 3000 human patients, i.e., this compound can be readily translated to the clinic for various neuroinflammatory diseases. OKN-007 is currently an investigational new drug as a possible therapeutic for glioblastomas (phase 2 clinical trial for recurrent glioblastoma (GBM) patients as a sole agent, and in phase 1b clinical trial in combination with temozolomide for newly diagnosed GBM patients). OKN-007 would be a suitable therapeutic candidate for neuroinflammatory diseases.

In the current study, we evaluated the effect of OKN-007 on neuroinflammatory-associated events in a LPS-induced encephalopathy rat model over a period of 6 weeks. A combination of MR techniques, including CE-MRI, pMRI, and ^{1}H-MRS and free radical–targeted mt-MRI were used to assess long-term neuroinflammation-associated alterations in BBB permeability, microvascularity, neurological metabolism, and free radical levels, respectively.

Materials and methods

Ethics statement

Animal experiments were performed with the approval and strict adherence to the policies of the Oklahoma Medical Research Foundation Institutional Animal Care and Use Committee, which specifically approved this study, with adherence to the *National Institutes of Health Guide for the Care and Use of Laboratory Animals*. All efforts were made to minimize suffering.

LPS exposure

Rats (Sprague-Dawley; 8–10 weeks old; male; $n = 30$) were exposed to LPS (10 mg/kg in 100 μL saline; i.p.). Controls were administered saline (same volume and route of administration as for LPS).

OKN-007 treatment

OKN-007 was administered 24 h following LPS exposure and continuously on a daily basis in the drinking water (18 mg/kg or 0.018% *w/v*; daily) until the animal

was euthanized at each time point. Water bottles were weighed daily, and it was established that rats generally consumed ~ 10 mg/kg of OKN-007 daily.

MRI methods—contrast-enhanced MRI, perfusion imaging, and MR spectroscopy

MRI experiments were done on a Bruker Biospec 7.0 Tesla/30-cm horizontal bore imaging system. Multiple brain [1]H-MR image slices were taken using a RARE multi-slice (repetition time (TR) 1.3 s, echo time (TE) 9 ms, 256 × 256 matrix, 4 steps per acquisition, 4 × 4 cm^2 field of view, 1.0-mm slice thickness) imaging sequence.

For contrast-enhanced MRI (CE-MRI), multi-slice spin echo T1-weighted images (TR = 1000.0 ms, TE = 14 ms, field of view (FOV) = 4 × 4 cm^2, averages = 2, slices = 16, matrix size = 256 × 256) were also performed and acquired before and 10, 20, and 30 min after intravenous contrast agent injection (Gd-DTPA, Magnevist, Bayer Inc., Wayne, NY, USA; 0.4 mmol/kg) (Towner et al. 2018). Regional assessments were made in the following regions: the cortex and hippocampus regarding MRI signal intensity measurements.

^{1}H-MRS was acquired using a PRESS (Point RE-solved SpectroScopy) sequence with a TE of 24.0 ms, a TR of 2500.0 ms, 512 averages, and a spectral width of 4006 Hz. A nonsuppressed MR spectrum was acquired beforehand by applying eddy current correction to maximize signal intensity and decrease the peak linewidths. Water was suppressed with a VAPOR (variable power radio frequency pulses and optimized relaxation delays) suppression scheme. In all cases, the peak width (full width at half maximum) of the water peak was less than 30 Hz following localized shimming, which was conducted by using the first- and second-order adjustments with Fastmap. A cubic voxel of 3.0 × 3.0 × 3.0 mm^3 was positioned in the rat brain. To analyze the MRS data, an in-house Mathematica program was used (version 6.0, Wolfram Research, Champaign, IL, USA). The spectra were scaled in ppm by calibrating against the water peak (4.78 ppm). The major brain metabolic peaks were identified as follows: N-acetylaspartate (NAA) at 2.02 ppm, choline (Cho) at 3.22 ppm, creatine (Cr) at 3.02 ppm, and myo-inositol at 3.53 ppm. The peak area measurements of the metabolites were used to calculate the following ratios: NAA to Cho (NAA/Cho), Cr to Cho (Cr/Cho), and Myo-Ins to Cho (Myo-Ins/Cho).

Arterial spin labeling (ASL) perfusion maps were obtained on a single axial slice of the brain located on the point of the rostro-caudal axis where the hippocampus had the largest cross-section. The imaging geometry was a 4 × 4 cm^2 FOV of 2 mm in thickness, with a single-shot echo-planar encoding over a 64 × 64 matrix. An echo time (TE) of 13.5 ms, a repetition time (TR) of 18 s, and an inversion time (TIR) of 26.0 ms were used, and images were not submitted to time averaging (Towner et al. 2018). To obtain perfusion contrast, the flow alternating inversion recovery scheme was used. Briefly, inversion recovery images were acquired using a slice-selective inversion of the same geometry as the imaging slice or a nonselective inversion slice concentric with the imaging slice with a slice package margin of 5.0 mm. For each type of inversion, 22 images were acquired with inversion times evenly spaced from 26.0 to 8426.0 ms (with an increment of 400 ms between each TIR). Relative cerebral blood flow (rCBF) values were obtained by drawing circular regions of interest (ROIs) (left and right regions) in the cortex and hippocampus regions of the brain. Negative ASL rCBF values were assumed to be zero.

For free radical–targeted MRI, rat brains were imaged at 0 (pre-contrast) and up to 120 min post-contrast agent injection. Rats were previously treated with DMPO (5,5-dimethyl-1-pyrroline-N-oxide) (100 mg diluted in 200 μL saline; i.p.; 3 × daily every 6 h for 3 days) to trap free radicals and subsequently injected intravenously with the anti-DMPO-albumin-Gd-DTPA-biotin contrast agent (200 μg anti-DMPO antibody/rat and 100 mg biotin-albumin-Gd-DTPA/rat) for in vivo free radical–targeted molecular MRI. T1-weighted images were obtained using a variable TR (repetition time) spin echo sequence (TR, 200–1600 ms; TE, 15 ms; NA, 2) (Towner et al. 2018). Pixel-by-pixel relaxation maps were reconstructed from a series of T1-weighted images using a nonlinear two-parameter fitting procedure. The T1 values of specified ROIs were computed from all the pixels in designated ROIs.

Statistical analyses

Statistical analyses were performed using GraphPad Prism 6 (GraphPad Prism 6 Software, San Diego, CA, USA). All p values < 0.05 were considered statistically significant. MRI signal intensities, rCBF values, and metabolite peak ratios ((NAA/Cho), (Cr/Cho), and (Myo-Ins/Cho)) were reported as means ± standard

deviations. For statistical analysis, Student t tests (independent-samples, two-tailed t test) were used to assess the differences between means of the LPS-exposed and saline-treated control rat brains and those that were untreated versus treated with OKN-007.

Results

OKN-007 restores LPS-induced blood-brain barrier permeability to normal

CE-MRI, which detects BBB permeability alterations, indicated a significant increase in MRI signal intensity (SI) due to the presence of Gd-DTPA in LPS-exposed rat brains at 24 h post-injection in the cerebral cortex ($p < 0.05$), and hippocampus ($p < 0.05$), compared with saline-treated controls (Fig. 1A, B). At longer time points (1 week and 6 weeks post-LPS), there was also a significant increase in BBB permeability in the cerebral cortex (0 < 0.05 for both time points), when compared with saline controls. In the hippocampus, there was a significance in the 6 weeks post-LPS group ($p < 0.05$), compared with controls. A significantly decreased MRI SI was also observed in the LPS rat brains treated with OKN-007 in the cerebral cortex ($p < 0.05$)(Fig. 1A), and hippocampus ($p < 0.05$) (Fig. 1B) 1 week after LPS injection, compared with LPS-exposed rat brains alone. For other time points, there was a trending decrease in relative MRI signal intensity, although not found to be significant to LPS exposure alone. These results indicate some restoration in BBB integrity with OKN-007 treatment.
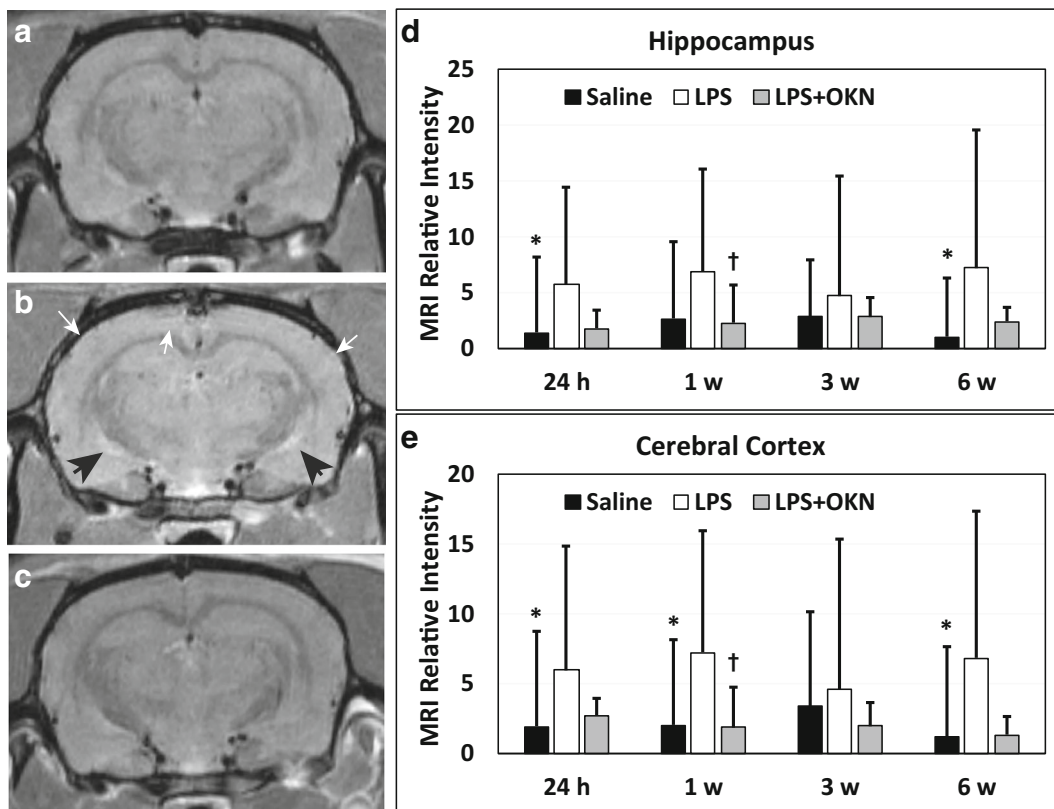

Fig. 1 OKN-007 restores BBB integrity in LPS-treated rat brains. Representative MR images of rat mid-brain regions for (A) saline, (B) LPS alone, or (C) LPS + OKN-007 treatment at 1 week post-LPS (or saline). Note highlighted hyperintensity regions in the LPS-exposed rat brain (panel B; white arrows: cortex; black arrows: lower hippocampal region). There were increased relative MRI signal intensities for LPS-treated brains, compared with saline-administered rat brains in the (D) hippocampus, and (E) cerebral cortex, at 24 h and 6 weeks post-LPS, and 1 week post-LPS in the cortex (*$p < 0.05$ for all). OKN-007 was able to significantly decrease relative MRI signal intensity, i.e., restore BBB, in the hippocampus and cerebral cortex at 1 week post-LPS in LPS + OKN-007-treated rat brains, compared with LPS exposure only (†$p < 0.05$ for both)

OKN-007 restores LPS-induced reduced brain tissue perfusion rates to normal

pMRI indicated that for the cortex and hippocampus regions, LPS-exposed rat brains had significantly decreased rCBF at all time points (1, 3, and 6 weeks post-LPS), compared with controls. Regarding a treatment effect from OKN-007, there was a restoration of rCBF in both the cerebral cortex and hippocampus regions at all time points (Fig. 2A, B) for the LPS-exposed rat brains treated with OKN-007, compared with LPS-exposed rat brains alone. These results strongly suggest
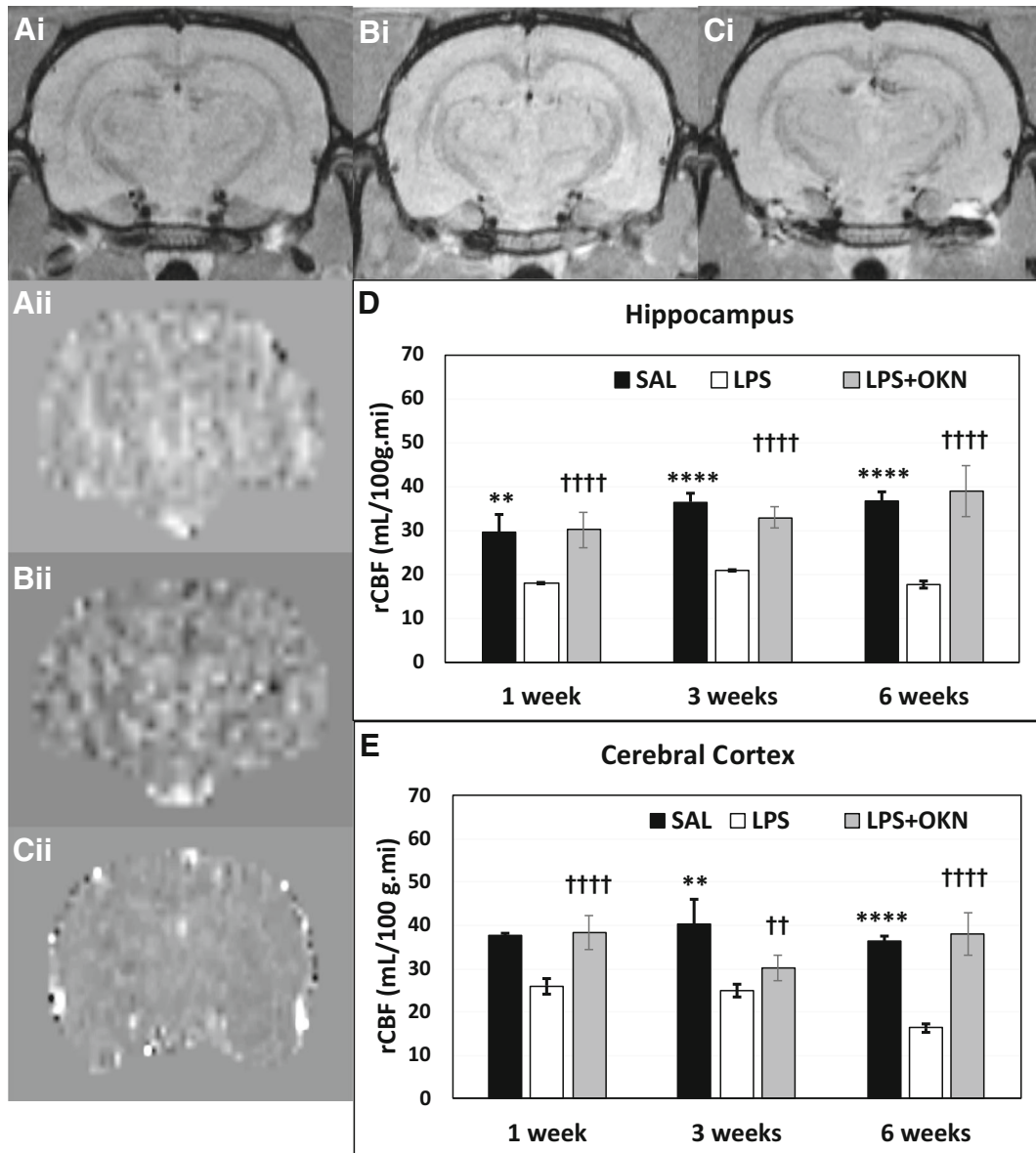
Fig. 2 OKN-007 restores brain vascularity to normal in LPS-exposed rat brains. Representative morphological MR images (i) and perfusion maps (ii) for saline (A), LPS (B), or LPS + OKN-007-treated (C) rat brains. LPS-treated rat brains have significantly decreased relative cerebral blood flow (rCBF) at 1–3 weeks in both the hippocampus (D) and cerebral cortex (E) regions post-LPS exposure (LPS versus saline: cerebral cortex (****$p < 0.0001$ at 1 and 6 weeks and **$p < 0.01$ at 3 weeks); hippocampus (**$p < 0.01$ at 1 weeks and ****$p < 0.0001$ at 3 and 6 weeks)). rCBF was found to be significantly restored by OKN-007 treatment in LPS-exposed rat brains in the cerebral cortex (††††$p < 0.0001$ at 1 and 6 weeks post-LPS and ††$p < 0.01$ at 3 weeks) and hippocampus (††††$p < 0.0001$ at all time points), when compared with LPS exposure alone

that OKN-007 restores vascularity, altered by LPS exposure, back to normal.

OKN-007 restores LPS-induced reduced brain metabolite levels to normal

The MRS data indicated that LPS-exposed rat brains had significantly decreased NAA/Cho metabolite ratios at 24 h ($p < 0.05$), 3 weeks ($p < 0.05$), and 6 weeks ($p < 0.05$) post-LPS injection; Cr/Cho ratios at 1, 3, and 12 weeks ($p < 0.05$ for all) post-LPS; and Myo-Ins/Cho ratios at 1 ($p < 0.05$), 3 ($p < 0.0001$), and 6 weeks ($p < 0.05$), compared with controls (Fig. 3). Cr/Cho ratios were also found to significantly decrease at 3 weeks post-LPS ($p < 0.01$), compared with controls.
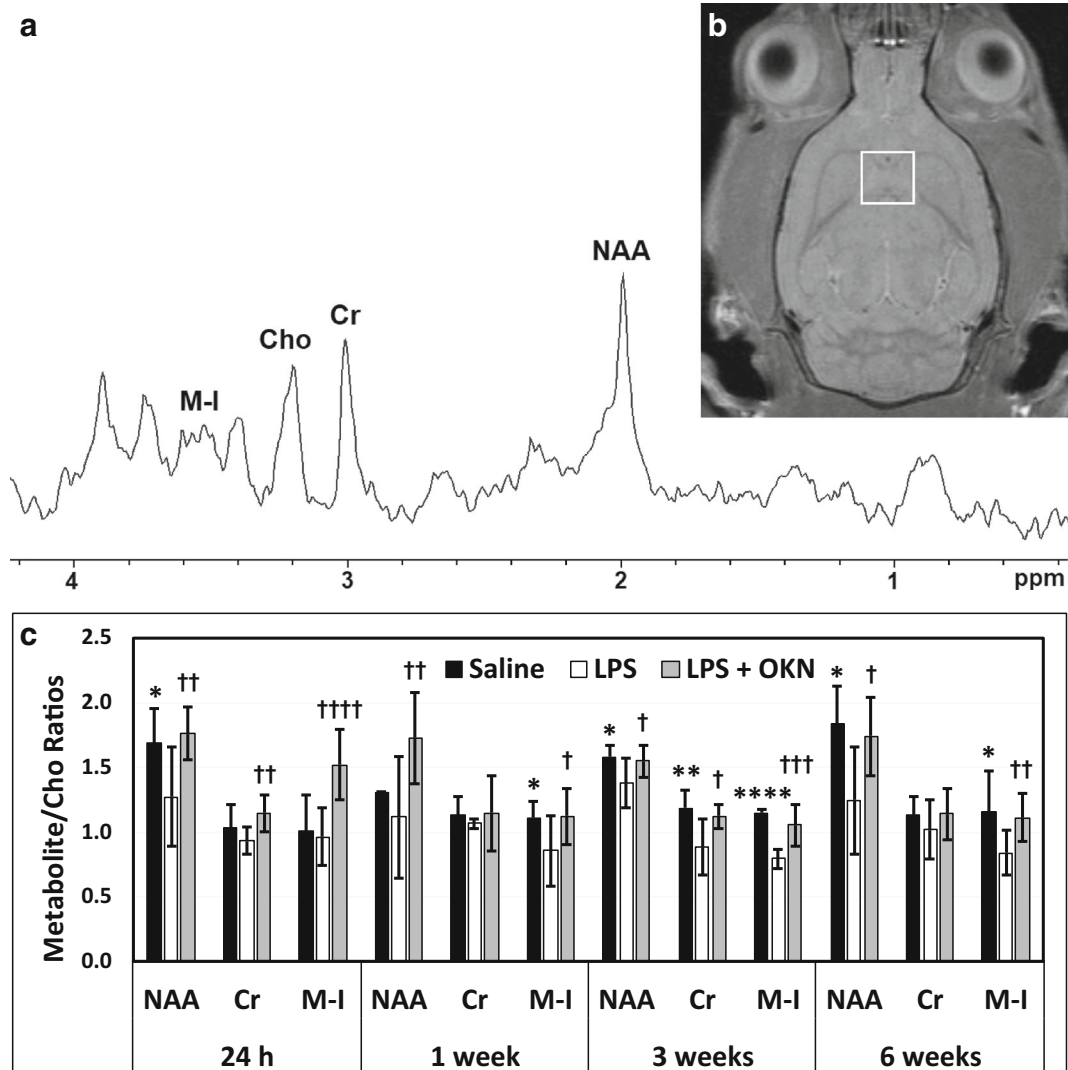

Fig. 3 OKN-007 restores brain metabolites to normal following LPS exposure. (A) Representative MR spectrum in a saline-treated rat brain at 1 week post-saline. (B) Representative MR image with depicted voxel obtained in hippocampal region (white square). (C) LPS-treated rat brains have decreased brain metabolites at various time points following LPS exposure. Metabolite/choline (Cho) ratios for NAA/Cho (24 h and 6 weeks post-LPS; *$p < 0.05$), Cr/Cho (3 weeks post-LPS; **$p < 0.01$), and Myo-Ins/Cho (1 week (*$p < 0.05$), 3 weeks (****$p < 0.0001$), and 6 weeks (*$p < 0.05$) post-LPS) are decreased when comparing LPS- and saline-administered rat brains. OKN-007 restores brain metabolites (NAA/Cho ratio at 24 h and 1 week (††$p < 0.01$ for both), as well as 3 and 6 weeks post-LPS (†$p < 0.05$ for both); Cr/Cho ratio at 24 h (††$p < 0.01$) and 3 weeks (†$p < 0.05$) post-LPS; and Myo-Ins/Cho ratio at 24 h (††††$p < 0.0001$), 1 week (†$p < 0.05$), 3 weeks (†††$p < 0.001$), and 6 weeks (††$p < 0.01$) post-LPS), when compared with LPS alone. Abbreviations: NAA = N-acetyl aspartate; Cr = total creatine; Cho = total choline; M-I = Myo-Inositol

OKN-007 treatment of LPS-exposed rat brains significantly restored all metabolites assessed (NAA, Cr, Myo-Ins/Cho ratios) at 24 h post-LPS, compared with LPS-exposed animals alone. At longer time points, OKN-007 was able to restore Myo-Ins at 1, 3, and 6 weeks post-LPS; NAA at 3 and 6 weeks post-LPS; and Cr at 3 weeks post-LPS, compared with LPS alone. These results indicate that OKN-007 can restore LPS-induced depleted brain metabolites to normal levels, particularly at longer time points.

OKN-007 reduces LPS-induced increased free radicals

The targeted free radical imaging approach indicated the detection of significantly increased trapped radical levels in LPS-exposed rat brains at both 24 h and 1 week post-LPS injection, compared with saline-treated controls (Fig. 4). OKN-007 treatment significantly decreased free radical levels at both 24 h and 1 week post-LPS, compared with LPS-exposed animals alone. These results indicate that OKN-007 can remove damaging free radicals following LPS exposure.
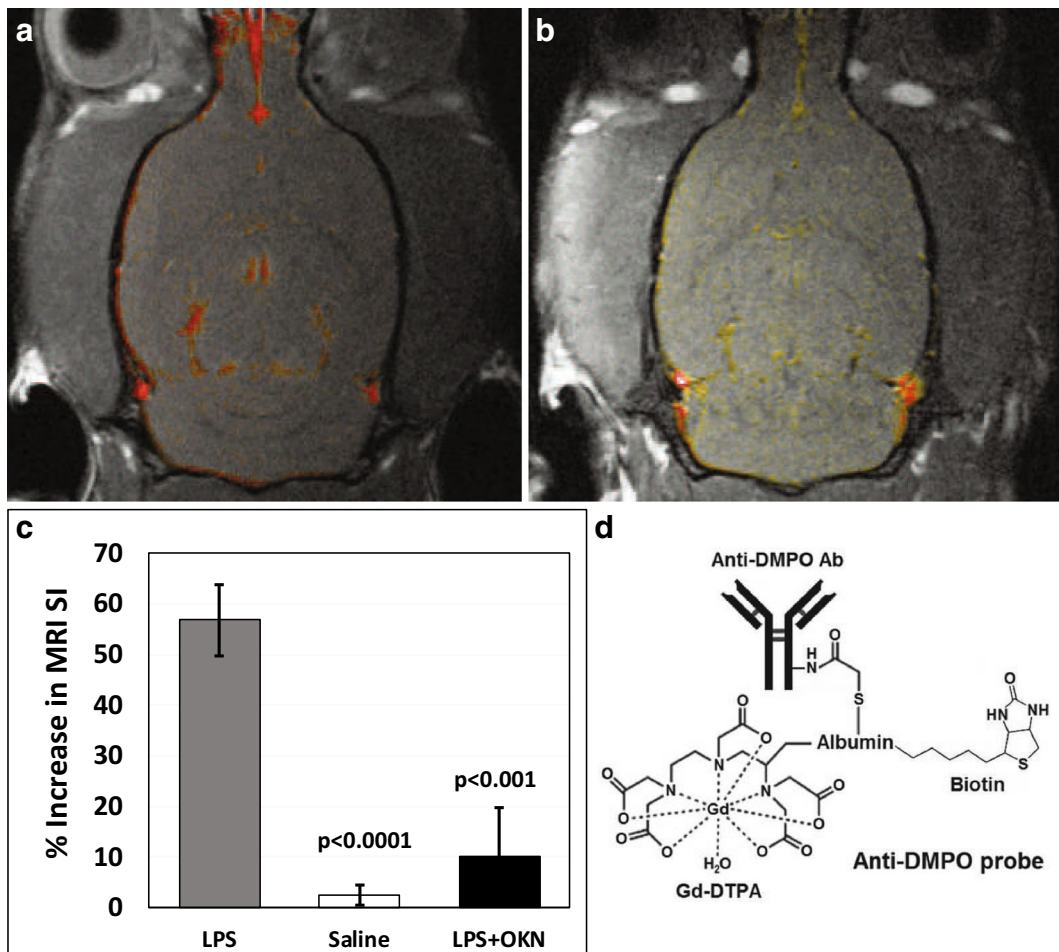
Fig. 4 OKN-007 reduces free radical levels in LPS-exposed rat brains. At 1 week post-LPS, there are increased free radical levels ($p < 0.0001$) compared with saline. Representative T1-weighted images overlaid with a post- minus a pre-contrast image following administration of the anti-DMPO probe that targets DMPO-trapped macromolecular radicals for (A) LPS-administered rat brains at 1 week post-LPS and (B) OKN-007 treatment following LPS exposure after 1 week. (C) MRI signal intensity percent (%) differences normalized to muscle graphs of LPS- and saline-administered rat brains given anti-DMPO probes at 1 week post-LPS, saline or LPS + OKN-007. There was a significant decrease in detection of DMPO-trapped radicals in the LPS + OKN-007-treated rat brains at 1 week ($p < 0.001$) post-LPS, compared with LPS alone. (D) Illustration of the anti-DMPO probe, which consists of Gd-DTPA, anti-DMPO antibody bound to albumin, and biotin

Discussion

Our findings indicated that CE-MRI, which detects BBB permeability alterations, can be assessed by measuring increased relative MRI signal intensities, due to the presence of the MRI contrast agent, Gd-DTPA. We were able to show a significant increase in the uptake of Gd-DTPA in LPS-exposed rat brains at 24 h, 1 week, and 6 weeks post-LPS exposure in the cerebral cortex ($p < 0.05$ for all) and at 24 h and 6 weeks post-LPS in the hippocampus ($p < 0.05$ for both), compared with saline-treated controls (see Fig. 1). With OKN-007 treatment of LPS-exposed rats, significantly decreased MRI SI was observed in both the cerebral cortex ($p < 0.05$) and hippocampus ($p < 0.05$) 1 week after LPS injection, compared with LPS-exposed animals alone. There was also a decreasing effect from the OKN-007 treatment for other time points, but these were not significant. Overall, OKN-007 does seem to restore BBB integrity following an LPS insult.

It is well known that LPS can disrupt the BBB (Wispelwey et al. 1988; Banks and Erickson 2010). It was previously reported that dynamic contrast-enhanced (DCE) MRI could be used to detect blood-brain barrier (BBB) breakdown 24 h following stereotaxic injection of LPS into the right striatum in rats but was found to be absent at 1 month post-LPS injection (Ory et al. 2015). In support of the Ory and co-worker study, our results did not detect a significant difference in BBB breakdown in either the cerebral cortex or the hippocampus at 3 weeks post-LPS exposure. However, at 6 weeks post-LPS, we did find a significant increase in BBB breakdown, compared with saline controls, indicating that there may be a long-term effect. Another group used multi-photon imaging to detect increased BBB dysfunction in LPS-exposed mice (Zhou et al. 2014). Of interest, it was established that Wip1 regulates LPS-induced neuroinflammation and BBB function via the sonic hedgehog signaling pathway (Zhen et al. 2017). It is also well documented that there is age-associated BBB impairment that contributes to a decline in neurological and cognitive functions (Erdő et al. 2017).

The cerebral cortex plays key roles in several brain functions, which includes memory, cognition, awareness, thought, language, attention, and consciousness (Shipp 2007). LPS exposure could possibly affect both short-term and long-term cognition, which we recently reported on (Kirk et al. 2019). The hippocampus is involved in both short-term and long-term memory (Squire 1992). We recently found that hippocampal memory is affected by LPS exposure (Kirk et al. 2019). Regarding altering BBB permeability, LPS exposure seems to affect both the cerebral cortex and hippocampus at relatively longer time points.

Regarding brain tissue vascular perfusion, there were a few interesting occurrences that we observed regarding OKN-007 treatment of LPS-exposed rat brains (see Fig. 2). For the cortex and hippocampus, there were both short-term (1 week post-LPS) and long-term (3 and 6 weeks) significant decreases in rCBF detected for LPS-exposed rat brains ($p < 0.01$ or more for the cortex and $p < 0.01$ or more for the hippocampus), compared with controls, which were reversed back to normal in both brain regions at all time points following OKN-007 treatment. Another reported study that assessed regional cerebral blood flow (CBF), measured by positron emission tomography (PET) using ^{18}F-fluorodeoxyglucose (^{18}F-FDG) in LPS-exposed rats, found CBF to decrease in the cortex (Semmler et al. 2008), which supported our findings. It is also known that changes in cerebral blood flow, release of inflammatory molecules, and metabolic alterations, associated with sepsis-associated encephalopathy (SAE), have been previously found to contribute to neuronal dysfunction and cell death (Semmler et al. 2008). From a human study, cerebral perfusion alterations and cognitive decline were observed in critically ill sepsis survivors (Pierrakos et al. 2017). Alterations in CBF are thought to represent a key component for the development of SAE (Taccone et al. 2013; Towner et al. 2018). It has also been reported that age-related cerebromicrovascular dysfunction plays an important role in the pathogenesis of dementia in the elderly (Toth et al. 2017; Tarantini et al. 2017). Aging has also been found to exacerbate the development of cerebral microbleeds (Sumbria et al. 2018).

Our MRS studies indicated that OKN-007 treatment of LPS-exposed rat brains had significantly restored some brain metabolites to normal levels. LPS exposure alone decreased NAA/Cho metabolite ratios at 24 h ($p < 0.05$), 3 weeks ($p < 0.05$), and 6 weeks ($p < 0.05$) post-LPS injection; Cr/Cho ratios at 3 weeks ($p < 0.01$) post-LPS; and Myo-Ins/Cho ratios at 1 ($p < 0.05$), 3 ($p < 0.0001$), and 6 weeks ($p < 0.05$), compared with controls (see Fig. 3). OKN-007 restored NAA/Cho ratios at all time points ($p < 0.5$ or less); Cr/Cho ratios at 24 h ($p < 0.01$) and 3 weeks ($p < 0.05$); and Myo-Ins/

Cho ratios at all time points ($p < 0.05$ or less) post-LPS, when compared with LPS exposure alone. Age-related decreases in NAA have also been recently reported in aging human adults using MRS (Maghsudi et al. 2019).

An antibody that recognizes macromolecular DMPO (5,5-dimethyl-pyrroline-N-oxide) spin adducts, regardless of the oxidative/reductive state of the trapped radical adducts, was developed by Mason et al. and coined immuno-spin trapping (IST) (Mason 2004; Ramirez and Mason 2005; Gomez-Mejiba et al. 2009, 2014; Khoo et al. 2015; Mason 2016). The spin trapping compound, DMPO, has been used for several decades to trap and stabilize free radical species. Our group extended the IST technique to an in vivo approach that involves the use of IST in conjunction with molecular-targeted magnetic resonance imaging (mt-MRI) (Towner et al. 2012, 2013a, 2013b, 2013c, 2015; Coutinho de Souza et al. 2015; Towner and Smith 2017). The spin trapping agent, DMPO, is used initially to trap free radicals in an oxidative stress–related disease model, and administration of a molecular magnetic resonance imaging (mMRI) probe, called the anti-DMPO probe, which combines an antibody against DMPO-radical adducts and a MRI contrast agent, is used to target the DMPO-trapped free radicals that can be detected by mMRI. The anti-DMPO probe includes an albumin-Gd-DTPA-biotin construct, where the anti-DMPO antibody is covalently linked to the cysteine residues of albumin, forming an anti-DMPO-adduct antibody-albumin-Gd-DTPA-biotin entity. The Gd-DTPA moiety acts as the MRI signaling component, which will increase MRI SI in a T1-weighted morphological MR imaging sequence and decrease T_1 relaxation in a T_1 map image. Both of these parameters, MRI SI or T_1 relaxation, can be used to assess the presence of the anti-DMPO probe in vivo.

In this study, free radical imaging indicated that OKN-007 treatment returned free radical levels to normal. Without OKN-007, the detection of significantly increased trapped radical levels in LPS-exposed rat brains was observed at both 24 h and 1 week post-LPS injection, compared with saline-treated controls (see Fig. 4). The free radical levels seem to be predominantly localized surrounding the hippocampal region. The OKN-007-treated LPS-exposed rat brains were found to have free radical levels that were similar to those detected in the negative control saline-treated group, i.e., close to baseline.

It was also reported by others that high levels of reactive oxygen species (ROS) were detected in a mouse LPS-induced SAE model (Zhou et al. 2014; Clement et al. 2010). In another study where a LPS-induced SAE mouse model was used, they showed not only high levels of ROS but also elevated malondialdehyde (MDA), tumor necrosis factor (TNF-α), and interleukin 1β (LI-1β), 8 h after LPS injection (Ning et al. 2017). It has also been found that free radical/ROS/RNS (reactive nitrogen species) involvement directly plays a role in the functional decline of aged brains (Poon et al. 2004). It has also been reported that oxidative stress plays a major role in cerebrovascular alterations related to neurodegenerations (Carvalho and Moreira 2018).

It is well established that systemic inflammation induces mitochondrial dysfunction, which leads to oxidative stress (Bozza et al. 2013; Lyu et al. 2015; Wang et al. 2014; Berg et al. 2011). Mitochondrial dysfunction was found to be associated with altered mitochondrial tyrosine kinase Src and protein phosphatase 1B (PTP1B) levels in a rat model of LPS-induced SAE (Lyu et al. 2015). In the same study, pretreatment of mitochondrial proteins with active PTP1B resulted in overproduction of ROS and decreased mitochondrial membrane potential (Lyu et al. 2015). It was also found that the mitochondrial function of the hippocampus was severely impaired, coupled with increased ROS, neuronal apoptosis, and inflammation, in a CLP-induced SAE mouse model (Wu et al. 2015). In this same study, they investigated the effects of a mitochondria-targeted peptide SS-31 on mitochondrial function and cognitive deficits and found that the peptide SS-1 protected mitochondrial integrity, reversed mitochondrial dysfunction, inhibited cytochrome c-related apoptosis, and diminished inflammation (Wu et al. 2015). It is also known that reactive oxygen and nitrogen species (RONS) lead to structural and functional modifications of cellular proteins and lipids, resulting in cellular dysfunction, such as impaired energy metabolism, altered cell signaling and cell cycle control, impaired cell transport processes, and dysfunctional biological activities, immune activation, and inflammation (Bozza et al. 2013). RONS can be involved in several disease processes as causative agents or result as an effect of the pathogenesis, including SAE. Microglia activation has also been reported to be associated with the secretion of nitric oxide, ROS, and matrix metalloproteinases (MMPs) that can all contribute to blood-brain barrier (BBB) and neuronal damage (Wu et al. 2015). Free radical–induced structural membrane damage also induces neuroinflammation (Berg et al. 2011). The formation of excessive

superoxide radicals also depletes ambient nitric oxide in the cerebrovascular bed (Berg et al. 2011). This results in the formation of peroxynitrite, which irreversibly inhibits the mitochondrial electron transport chain, resulting in an increase in mitochondrial release of free radicals, and leads to mitochondrial dysfunction and neuronal bioenergetics failure (Berg et al. 2011). Additionally, free radicals trigger apoptosis via altering intracellular calcium homeostasis in brain regions such as the cerebral cortex and hippocampus, further exacerbating local inflammatory responses further (Berg et al. 2011).

We have previously shown that OKN-007 is able to downregulate expression of the lipopolysaccharide binding protein (LBP) gene in a rat glioma model (Towner et al. 2019) and possibly could be one of the mechanisms of action for the therapeutic response elicited by OKN-007 in the LPS-induced neuroinflammatory model. LBP is a soluble acute-phase protein that binds to bacterial LPS to elicit immune responses by presenting the LPS to important cell surface pattern recognition receptors called CD14 and TLR4 (Tsukamoto et al. 2018). Preliminary RNA-seq data comparing LPS-exposed and saline-treated rat brains 1 week post-LPS indicates that LBP is upregulated 3.84-fold more in LPS rat brains, compared with saline controls.

There is compelling evidence that systemic inflammation coupled with aging may exacerbate cognitive decline (Sun et al. 2015; Yamanaka et al. 2017). Our group has also recently shown that LPS induces amyloid-β and phosphorylated-tau (p-tau) formation in rat brains 1 week following LPS exposure (Wang et al. 2018). Both amyloid-β and p-tau are known to increase in Alzheimer's disease (AD) (Jacobs et al. 2019; Timmers et al. 2019) and could also be associated with aging (Hernàndez-Zimbrón et al. 2017). We anticipate that OKN-007 may be able to alleviate long-term neuroinflammation and cognitive decline in aged rodents and are planning these future studies.

Conclusions

In a rat LPS endotoxemia model, OKN-007 was found to reverse neuroinflammatory indications that were induced by LPS exposure. MRI approaches were used to conclusively demonstrate increased BBB permeability, decreased brain relative cerebral blood flow, decreased brain metabolites, and increased free radical levels, indicative of oxidative damage, from LPS exposure, that were all effectively restored to near normal following OKN-007 treatment. OKN-007 seems to be a promising agent that could treat long-term neuroinflammation and could be effective for various neuroinflammatory diseases and even perhaps age-associated neuroinflammation.

Compliance with ethical standards   Animal experiments were performed with the approval and strict adherence to the policies of the Oklahoma Medical Research Foundation Institutional Animal Care and Use Committee, which specifically approved this study, with adherence to the *National Institutes of Health Guide for the Care and Use of Laboratory Animals*.

References

Banks WA, Erickson MA (2010) The blood-brain barrier and immune function and dysfunction. Neurobiol Dis 37:26–32

Berg RM, Moller K, Bailey DM (2011) Neuro-oxidative-nitrosative stress in sepsis. J Cereb Blood Flow Metab 31:1532–1544

Bettio LEB, Rajendran L, Gil-Mohapel J (2017) The effects of aging in the hippocampus and cognitive decline. Neurosci Biobehav Rev 79:66–86

Bozza FA, D'Avila JC, Ritter C, Sonneville R, Sharshar T, Dal-Pizzol F (2013) Bioenergetics, mitochondrial dysfunction, and oxidative stress in the pathophysiology of septic encephalopathy. Shock 39:10–16

Carvalho C, Moreira PI (2018) Oxidative stress: a major player in cerebrovascular alterations associated to neurodegenerative events. Front Physiol 9:806

Clausen F, Marklund N, Lewen A, Hillered L (2008) The nitrone free radical scavenger NXY-059 is neuroprotective when administered after traumatic brain injury in the rat. J Neurotrauma 25:1449–1457

Clement HW, Vasquez JF, Sommer O, Heiser P, Morawietz H, Hopt U, Schulz E, von Dobschutz E (2010) Lipopolysaccharide-induced radical formation in the striatum is abolished in Nox2 gp91phox-deficient mice. J Neural Transm (Vienna) 117(1):13–22

Coutinho de Souza P, Smith N, Atolagbe O, Ziegler J, Nijoku C, Lerner M, Ehrenshaft M, Mason RP, Meek B, Plafker SM, Saunders D, Mamedova N, Towner RA (2015) OKN-007 decreases free radical levels in a preclinical F98 rat glioma model. Free Radic Biol Med 87:157–168

Culot M, Mysiorek C, Renftel M, Roussel BD, Hommet Y, Vivien D, Cecchelli R, Fenart L, Berezowski V, Dehouck MP, Lundquist S (2009) Cerebrovascular protection as a possible mechanism for the protective effects of NXY-059 in preclinical models: an in vitro study. Brain Res 1294:144–152

Cunningham C, Hennessy E (2015) Co-morbidity and systemic inflammation as drivers of cognitive decline: new experimental models adopting a broader paradigm in dementia research. Alzheimers Res Ther 7:33

Edenius C, Strid S, Borga O, Breitholtz-Emanuelsson A, Vallen KL, Fransson B (2002) Pharmacokinetics of NXY-059, a nitrone-based free radical trapping agent, in healthy young and elderly subjects. J Stroke Cerebrovasc Dis 11:34–43

Erdő F, Denes L, de Lange E (2017) Age-associated physiological and pathological changes at the blood-brain barrier: a review. J Cereb Blood Flow Metab 37:4–24

Floyd RA, Kopke RD, Choi CH, Foster SB, Doblas S, Towner RA (2008) Nitrones as therapeutics. Free Radic Biol Med 45(10): 1361–1374

Floyd RA, Chandru HK, He T, Towner R (2011) Anti-cancer activity of nitrones and observations on mechanism of action. Anti Cancer Agents Med Chem 11(4):373–379

Floyd RA, Castro Faria Neto HC, Zimmerman GA, Hensley K, Towner RA (2013) Nitrone-based therapeutics for neurodegenerative diseases. Their use alone or in combination with lanthionines. Free Radic Biol Med 62:145–156

Gomez-Mejiba SE, Zhai Z, Akram H, Deterding LJ, Hensley K, Smith N, Towner RA, Tomer KB, Mason RP, Ramirez DC (2009) Immuno-spin trapping of protein and DNA radicals: "tagging" free radicals to locate and understand the redox process. Free Radic Biol Med 46:853–865

Gomez-Mejiba SE, Zhai Z, Della-Vedova MC, Muñoz MD, Chatterjee S, Towner RA, Hensley K, Floyd RA, Mason RP, Ramirez DC (2014) Immuno-spin trapping from biochemistry to medicine: advances, challenges, and pitfalls. Focus on protein-centered radicals. Biochim Biophys Acta 1840(2):722–729

Hernández-Zimbrón LF, Perez-Hernández M, Torres-Romero A, Gorostieta-Salas E, Gonzalez-Salinas R, Gulias-Cañizo R, Quiroz-Mercado H, Zenteno E (2017) Markers of Alzheimer's disease in primary visual cortex in normal aging in mice. Biomed Res Int 2017(3706018):1–10

Jacobs KR, Lim CK, Blennow K, Zetterberg H, Chatterjee P, Martins RN, Brew BJ, Guillemin GJ, Lovejoy DB (2019) Correlation between plasma and CSF concentrations of kynurenine pathway metabolites in Alzheimer's disease and relationship to amyloid-β and tau. Neurobiol Aging 80:11–20

Khoo NK, Cantu-Medellin N, St Croix C, Kelley EE (2015) In vivo immuno-spin trapping: imaging the footprints of oxidative stress. Curr Protoc Cytom 74:12.42.1–12.4211

Kirk RA, Kesner RP, Wang L-M, Wu Q, Towner RA, Hoffman JM, Morton KA (2019) Lipopolysaccharide exposure in a rat sepsis model results in hippocampal amyloid-β plaque and phosphorylated tau deposition and corresponding behavioral deficits. GeroScience. (in press)

Kuroda S, Tsuchidate R, Smith ML, Maples KR, Siesjo BK (1999) Neuroprotective effects of a novel nitrone, NXY-059, after transient focal cerebral ischemia in the rat. J Cereb Blood Flow Metab 19:778–787

Lyden PD, Shuaib A, Lees KR, Davalos A, Davis SM, Diener HC, Grotta JC, Ashwood TJ, Hardemark HG, Svensson HH, Rodichok L, Wasiewski WW, Ahlberg G (2007) Safety and tolerability of NXY-059 for acute intracerebral hemorrhage: the CHANT trial. Stroke 38:2262–2269

Lyu J, Zheng G, Chen Z, Wang B, Tao S, Xiang D, Xie M, Huang J, Liu C, Zeng Q (2015) Sepsis-induced brain mitochondrial dysfunction is associated with altered mitochondrial Src and PTP1B levels. Brain Res 1620:130–138

Maghsudi H, Schütze M, Maudsley AA, Daak M, Lanfermann H, Ding XQ (2019) Age-related brain metabolic changes up to the seventh decade in healthy humans: whole-brain magnetic resonance spectroscopic imaging study. Clin Neuroradiol. https://doi.org/10.1007/s00062-019-00814.z

Mason RP (2004) Using anti-5,5-dimethyl-1-pyrroline N-oxide (anti-DMPO) to detect protein radicals in time and space with immuno-spin trapping. Free Radic Biol Med 36:1214–1223

Mason RP (2016) Imaging free radicals in organelles, cells, tissue, and in vivo with immuno-spin trapping. Redox Biol 8:422–429

Murray C, Sanderson DJ, Barkus C, Deacon RM, Rawlins JN, Bannerman DM, Cunningham C (2012) Systemic inflammation induces acute working memory deficits in the primed brain: relevance for delirium. Neurobiol Aging 33(603–16): e3

Ning Q, Liu Z, Wang X, Zhang R, Zhang J, Yang M, Sun H, Han F, Zhao W, Zhang X (2017) Neurodegenerative changes and neuroapoptosis induced by systemic lipopolysaccharide administration are reversed by dexmedetomidine treatment in mice. Neurol Res 39(4):357–366

Oedekoven CS, Jansen A, Keidel JL, Kircher T, Leube D (2015) The influence of age and mild cognitive impairment on associative memory performance and underlying brain networks. Brain Imaging Behav 9(4):776–789

Ory D, Planas A, Dresselaers T, Gsell W, Postnov A, Celen S, Casteels C, Himmelreich U, Debyser Z, Van Laere K, Verbruggen A, Bormans G (2015) PET imaging of TSPOI in a rat model of local neuroinflammation induced by intracerebral injection of lipopolysaccharide. Nucl Med Biol 42(10):753–761

Pierrakos C, Attou R, Decorte L, Velissaris D, Cudia A, Gottignies P, Devriendt J, Tsolaki M, De Bels D (2017) Cerebral perfusion alterations and cognitive decline in critically ill sepsis survivors. Acta Clin Belg 72(1):39–44

Poon HF, Calabrese V, Scapagnini G, Butterfield DA (2004) Free radicals and brain aging. Clin Geriatr Med 20:329–359

Ramirez DC, Mason RP (2005) Immuno-spin trapping: detection of protein-centered radicals. Curr Protoc Toxicol 17:17

Semmler A, Hermann S, Mormann F, Weberpals M, Paxian SA, Okulla T, Schafers M, Kummer MP, Klockgether T, Heneka MT (2008) Sepsis causes neuroinflammation and concomitant decrease of cerebral metabolism. J Neuroinflammation 5: 38

Shipp S (2007) Structure and function of the cerebral cortex. Curr Biol 17(12):R443–R449

Sumbria RK, Grigoryan MM, Vasilevko V, Paganini-Hill A, Kilday K, Kim R, Cribbs DH, Fisher MJ (2018) Aging exacerbates development of cerebral microbleeds in a mouse model. J Neuroinflammation 15:69

Sun J, Zhang S, Zhang X, Zhang X, Dong H, Qian Y (2015) IL-17A is implicated in lipopolysaccharide-induced neuroinflammation and cognitive impairment in aged rats via microglial activation. J Neuroinflammation 12:165

Taccone FS, Scolletta S, Franchi F, Donadello K, Oddo M (2013) Brain perfusion in sepsis. Curr Vasc Pharmacol 11(2):170–186

Tarantini S, Tran CHT, Gordon GR, Ungvari Z, Csiszar A (2017) Impaired neurovascular coupling in aging and Alzheimer's disease: contribution of astrocyte dysfunction and endothelial impairment to cognitive decline. Exp Gerontol 94:52–58

Timmers M, Tesseur I, Bogert J, Zetterberg H, Blennow K, Börjesson-Hanson A, Baquero M, Boada M, Randolph C, Tritsmans L, Van Nueten L, Engelborghs S, Streffer JR (2019) Relevance of the interplay between amyloid and tau for cognitive impairment in early Alzheimer's disease. Neurobiol Aging 79:131–141

Toth P, Tarantini S, Csiszar A, Ungvari Z (2017) Functional vascular contributions to cognitive impairment and dementia: mechanisms and consequences of cerebral autoregulatory dysfunction, endothelial impairment, and neurovascular uncoupling in aging. Am J Physiol Heart Circ Physiol 312(1):H1–H20

Towner R, Smith N (2017) *In vivo* and *in situ* detection of macromolecular free radicals using immune-spin trapping and molecular MRI. Antioxid Redox Signal 28(15):1404–1415

Towner RA, Smith N, Saunders D, Henderson M, Downum K, Lupu F, Silasi-Mansat R, Ramirez DC, Gomez-Mejiba SE, Bonini MG, Ehrenshaft M, Mason RP (2012) *In vivo* imaging of immuno-spin trapped radicals with molecular MRI in a mouse diabetes model. Diabetes 61:2405–2413

Towner RA, Garteiser P, Bozza F, Smith N, Saunders D, d'Avila JCP, Magno F, Oliveira MF, Ehrenshaft M, Lupu F, Silasi-Mansat R, Ramirez DC, Gomez-Mejiba SE, Mason RP, Faria-Neto HCC (2013a) *In vivo* detection of free radicals in mouse septic encephalopathy using molecular MRI and immuno-spin-trapping. Free Radica Biol Med 65:828–837

Towner RA, Smith N, Saunders D, De Souza PC, Henry L, Lupu F, Silasi-Mansat R, Ehrenshaft M, Mason RP, Gomez-Mejiba SE, Ramirez DC (2013b) Combined molecular MRI and immuno-spin-trapping for *in vivo* detection of free radicals in orthotopic mouse GL261 gliomas. Biochim Biophys Acta 1832:2153–2161

Towner RA, Smith N, Saunders D, Lupu F, Silasi-Mansat R, West M, Ramirez DC, Gomez-Mejiba SE, Bonini MG, Mason RP, Ehrenshaft M, Hensley K (2013c) *In vivo* detection of free radicals using molecular MRI and immuno-spin-trapping in a mouse model for amyotrophic lateral sclerosis (ALS). Free Radic Biol Med 63:351–360

Towner RA, Smith N, Saunders D, Carrizales J, Lupu F, Silasi-Mansat R, Ehrenshaft M, Mason RP (2015) *In vivo* targeted molecular magnetic resonance imaging of free radicals in diabetic cardiomyopathy within mice. Free Radic Res 49:1140–1146

Towner RA, Saunders D, Smith N, Towler W, Cruz M, Do S, Maher JE, Whitaker K, Lerner M, Morton KA (2018) Assessing long-term neuroinflammatory responses to encephalopathy using MRI approaches in a rat endotoxemia model. GeroScience 40(1):49–60

Towner RA, Smith N, Saunders D, Brown CA, Cai X, Ziegler J, Mallory S, Dozmorov MG, Coutinho De Souza P, Wiley G, Kim K, Kang S, Kong DS, Kim YT, Fung KM, Wren JD, Battiste J (2019) OKN-007 increases temozolomide (TMZ) sensitivity and suppresses TMZ-resistant glioblastoma (GBM) tumor growth. Transl Oncol 12(2):320–335

Tsukamoto H, Takeuchi S, Kubota K, Kobayashi Y, Kozakai S, Ukai I, Shichiku A, Okubo M, Numasaki M, Kanemitsu Y, Matsumoto Y, Nochi T, Watanabe K, Aso H, Tomioka Y (2018) Lipopolysaccharide (LPS)-binding protein stimulates CD14-dependent toll-like receptor 4 internalization and LPS-induced TBK1-IKKε-IRF3 axis activation. J Biol Chem 293(26):10186–10201

Wang Y, Chen Z, Zhang Y, Fang S, Zeng Q (2014) Mitochondrial biogenesis of astrocytes is increased under experimental septic conditions. Chin Med J 127(10):1837–1842

Wang LM, Wu Q, Kirk RA, Horn KP, Ebada Salem AH, Hoffman JM, Yap JT, Sonnen JA, Towner RA, Bozza FA, Rodrigues RS, Morton KA (2018) Lipopolysaccharide endotoxemia induces amyloid-β and p-tau formation in the rat brain. Am J Nucl Med Mol Imaging 8(2):86–99

Wemer J, Cheng YF, Nilsson D, Reinholdsson I, Fransson B, Vallen KL, Nyman L, Eriksson C, Bjorck S, Schulman S (2006) Safety, tolerability and pharmacokinetics of escalating doses of NXY-059 in healthy young and elderly subjects. Curr Med Res Opin 22:1813–1823

Wispelwey B, Lesse AJ, Hansen EJ, Scheld WM (1988) Haemophilus influenza lipopolysaccharide-induced blood brain barrier permeability during experimental meningitis in the rat. J Clin Invest 82:1339–1346

Wu J, Zhang M, Hao S, Jia M, Ji M, Qui L, Sun X, Yang J, Li K (2015) Mitochondria-targeted peptide reverses mitochondrial dysfunction and cognitive deficits in sepsis-associated encephalopathy. Mol Neurobiol 52(1):783–791

Yamanaka D, Kawano T, Nishigaki A, Aoyama B, Tateiwa H, Shigematsu-Locatelli M, Locatelli FM, Yokoyama M (2017) Preventive effects of dexmedetomidine on the development of cognitive dysfunction following systemic inflammation in aged rats. J Anesh 31:25–35

Zhen H, Zhao L, Ling Z, Kuo L, Xue X, Feng J (2017) Wip1 regulates blood-brain barrier function and neuroinflammation induced by lipopolysaccharide via the sonic hedgehog signaling signaling pathway. Mol Immunol 93:31–37

Zhou T, Zhao L, Zhan R, He Q, Tong Y, Tian X, Wang H, Zhang T, Fu Y, Sun Y, Xu F, Guo X, Fan D, Han H, Chui D (2014) Blood-brain barrier dysfunction in mice induced by lipopolysaccharide is attenuated by dapsone. Biochem Biophys Res Commun 453(3):419–424